

# Performance evaluation of a continuous flow immobilized rotating tube photocatalytic reactor (IRTPR) immobilized with TiO<sub>2</sub> catalyst for azo dye degradation

Rahul A. Damodar, T. Swaminathan \*

*Department of Chemical Engineering, Indian Institute of Technology Madras, Chennai 600036, Tamilnadu, India*

Received 11 October 2007; received in revised form 17 December 2007; accepted 4 January 2008

## Abstract

Photocatalytic oxidation is becoming an attractive technique for the degradation of hazardous organic contaminants. Reactor design plays an important role in the treatment efficiency. A novel immobilized photocatalytic reactor presented in this paper, consists of TiO<sub>2</sub> coated rotating PVC tubes in a continuous flow reactor; irradiated with UV lamps. Using reactors in series approach, the effects of key parameters—initial dye concentration, rotational speed, pH and flow rate, on color removal were evaluated for reactive red dye. Low initial concentration and acidic pH favored the dye removal. Rate of color removal increased with speed initially but remained constant at higher speed. Though the effect of flow rate was complex, in combination with initial concentration it had a significant effect on the energy consumption. Langmuir–Hinshelwood type kinetic model fitted the decolorization kinetic well and the rate constants were evaluated. 90–99.99% color removal and 55–70% TOC removal were obtained depending on operating conditions.

© 2008 Elsevier B.V. All rights reserved.

*Keywords:* Photocatalysis; TiO<sub>2</sub>; Photoreactor; Catalyst immobilization; AOP; Azo dye degradation; Decolorization; Rotating tube

## 1. Introduction

Heterogeneous photocatalysis has proved to be an effective treatment method for removal of toxic pollutants from industrial wastewaters owing to its ability to convert them into innocuous end products such as CO<sub>2</sub>, H<sub>2</sub>O and mineral acids. The application of photocatalysis for oxidation of several model pollutants has been experimentally verified [1–5]. Photocatalysis has also been found to treat nuisance odors and other hazardous organic pollutants from contaminated waste gases [2,6]. Heterogeneous photocatalysis, one of the advanced oxidation processes (AOP), uses certain metal oxides that upon adsorption of UV radiation, readily generate hydroxyl radicals which are the most reactive species having highest oxidation potential capable of breaking complex organic bonds. Although this field has been an active area of scientific research, its implementation in large scale has not been successful so far. The main reason for this is the slow development of practical photocatalytic systems that can be used efficiently and economically for the decontamination of water in

large-scale application [7]. Various photocatalytic reactor configurations have been employed in photodegradation process in laboratory scale, but very few have been commercialized.

There are two types of heterogeneous photoreactors, one in which the TiO<sub>2</sub> is in the form of a suspension or slurry and other in which it is immobilized on a solid surface. Both reactors offer different advantages. Most of the early photoreactors have used a suspension of TiO<sub>2</sub>, since it offers high surface area for reaction and almost no mass transfer limitation. But with slurry systems, some sort of recovery step is necessary to separate and reuse the catalyst. Though the efficiency of the immobilized system may be less than that of the slurry system, the catalyst can be used continuously for long time [8]. Many alternatives have been proposed in last few years, where researchers have tried a variety of support materials and coating methods [9].

Light absorption is an additional factor that has to be considered in the design of photoreactors. Rate of initiation step (i.e. electron–hole formation) in photochemical reaction is directly dependent on the radiation intensity. The efficiency of the reactor depends on the amount of catalyst, which is actually getting activated on exposure to light, and determines the treatment capacity of the reactor [10–13]. A high degree of mass transfer to improve reactant catalyst interactions and to improve oxygen

\* Corresponding author. Tel.: +91 44 22574166; fax: +91 44 22574152.  
E-mail address: tswami@iitm.ac.in (T. Swaminathan).

uptake at gas liquid interface is another requirement for practical applications [3].

Considering these requirements a new reactor based on the thin film concept was designed. It uses rotating surfaces coated with  $\text{TiO}_2$ , which are partially immersed in continuously flowing wastewater. The rotation of the immobilized surface allows the formation of a thin film of dye solution over the catalyst surface. This enables efficient penetration of UV radiation and good mixing and mass transfer of oxygen from air. The reactor is capable of utilizing both direct and diffuse portion of solar radiation. This paper discusses the results of a study on the evaluation of this novel photoreactor with immobilized  $\text{TiO}_2$  catalyst for azo dye degradation.

## 2. Material and methods

### 2.1. Materials

#### 2.1.1. Chemicals

Reactive red dye ( $\text{C}_{18}\text{H}_{11}\text{N}_8\text{O}_{10}\text{S}_3\text{ClNa}_3$ ,  $\lambda_{\text{max}} = 545 \text{ nm}$ ) commercial grade was purchased from TMR Chemicals & Co, Erode, India. All other chemical used in the experiments were of reagent grade. Titanium dioxide ( $\text{TiO}_2$ ) (pure anatase, BET surface area  $15 \text{ m}^2/\text{g}$ ) was supplied by CDH, India.

#### 2.1.2. Immobilized rotating tube photocatalytic reactor (IRTPR)

The schematic diagram of experimental reactor setup is shown in Fig. 1. The reactor consisted of a rectangular acrylic tank divided into equal sized cells. Each cell housed a PVC tube of 63 mm o.d., 46 cm length closed at both end and coated with  $\text{TiO}_2$ . The reactor was divided in to two equal halves R1 and R2 (as shown in Fig. 1) having the same volume ( $1.5 \text{ l}$ ), surface area (5 tubes,  $0.23 \text{ m}^2$ ) and also equal light distribution. The tubes were supported by shafts and held by bearings on both ends. All the tubes were simultaneously rotated using a V-belt through a variable speed DC-motor. The reactor was designed to give zigzag flow path for liquid in the reactor.

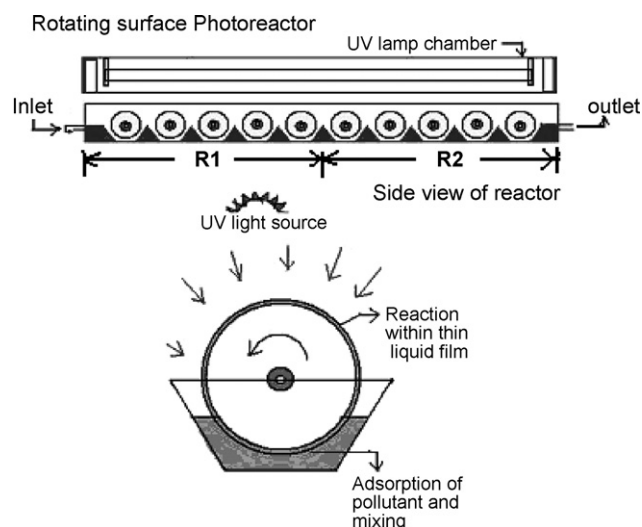


Fig. 1. Schematic of immobilized rotating tube photocatalytic reactor (IRTPR).

#### 2.1.3. UV source

The UV lamp house was made from rectangular metal sheet box with three low-pressure Hg UV lamps (30 W Philips UV-C) emitting predominantly at 254 nm wavelength. Two cooling fans were provided at both ends, for cooling the UV tubes and for circulation of air that will help in the transfer of oxygen to the liquid film. The inside of UV lamp house was covered with a polished reflector sheet to get good distribution of UV light over the entire surface.

### 2.2. Methods

#### 2.2.1. Coating method

A smooth paste of  $\text{TiO}_2$  was prepared by sonicating a slurry of 10 g of  $\text{TiO}_2$  in 1% Polyvinyl alcohol solution. The PVC tubes were washed with water initially and the  $\text{TiO}_2$  paste was applied on the wet surface as a thin layer using a smooth paint brush. The coated tubes were dried at ambient temperature and the procedure was repeated till a uniform coating was obtained. The tubes were rotated in distilled water for 1 h to remove loosely bound  $\text{TiO}_2$ . The coated surface was finally dried for 6 h at  $60^\circ\text{C}$  in a hot air oven.

#### 2.2.2. Continuous mode experimental studies in IRTPR

Studies were carried out in continuous mode using  $\text{TiO}_2$  coated IRTPR to study the degradation pattern of an azo dye, Reactive Red, at different initial concentrations, pH and flow rates. The dye solution of desired concentration was fed to the first reactor (R1) inlet and samples of the reaction medium were withdrawn at regular intervals at the end of each reactor R1 and R2. Samples were analyzed for residual dye concentration using a UV-vis spectrophotometer (Shimadzu, UV-1601PC), Total organic carbon (TOC-1200 Euroglass), pH, and conductivity.

## 3. Results and discussion

Heterogeneous photocatalysis plays a major role in detoxifying hazardous pollutants to innocuous end products. The rate and extent of photocatalytic degradation process is affected by variables such as initial dye concentration, pH, light intensity, flow rate, rotational speed, etc. The effects of some of these variables were studied in a continuous mode using IRTPR connected in series. Preliminary studies showed very poor color removal (5.2%) with UV irradiation without catalyst for nearly 5 h and less than 7% by adsorption on catalyst alone without UV irradiation.

The dye solution of desired concentration was fed to the first reactor (R1) inlet and the treated effluent was collected at the end of second reactor (R2). When a batch volume was completed, the effluent collected was again fed to first reactor. This procedure was repeated till complete color removal was obtained. Through this procedure, the numbers of reactors required in series were obtained. Fig. 2 shows the concentration of reactive red dye at each reactor outlet as a function of time. The figure also shows that the steady state was achieved within 90 min in all the experiments and nearly 6 reactors were required for complete color removal. The extent of color removal decreased in each reactor.

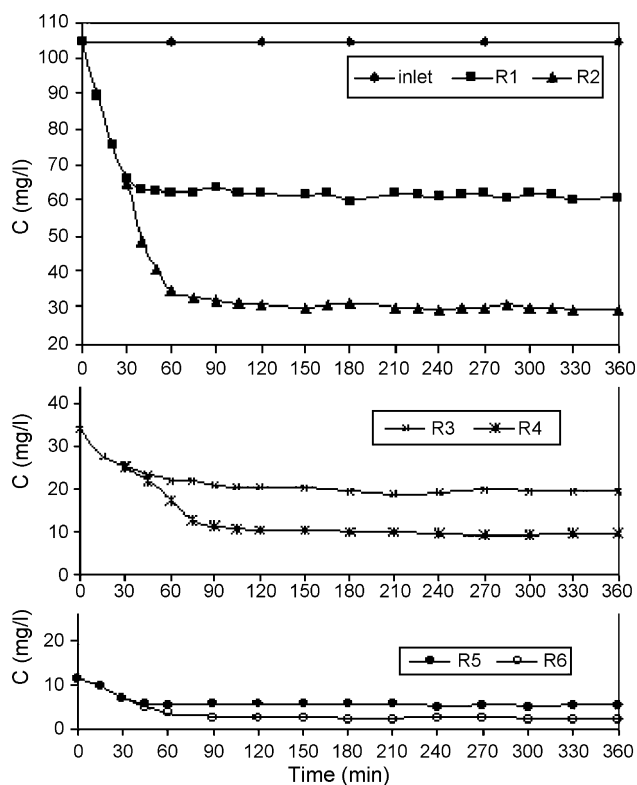


Fig. 2. Color removal pattern of reactive red dye (pH 5, flow rate—50 ml/min, dye concentration—100 mg/l, speed—25 rpm).

### 3.1. Effect of rotational speed

One of most commonly encountered problems with immobilized photoreactor configuration is mass transfer limitation in laminar flow region due to liquid film resistance. Photocatalysis is a surface phenomenon and the degradation occurs on the surface of catalyst. Therefore a continuous rapid exchange of pollutant across solid–liquid interface is needed. The tube rotational speed is a key factor, which determines the film thickness of the liquid carried by the tube, which in turn determines the mass transfer coefficient. It also influences the extent of oxygen entrainment in the liquid film carried by the tube [7,14–15]. Since rotation of tubes creates mixing and turbulence across solid–liquid interface, it improves the mass transfer of pollutant over the catalyst surface. Variation in film thickness also indirectly affects the UV light penetration on the surface of catalyst. As rotational speed increases, the exposure time decreases but at the same time the number of exposures increases (Table 1).

Table 1  
Relationship between rotational speed and exposure time

| Speed (rpm) | Exposure time/rotation (s) | Number of rotations ( $\text{min}^{-1}$ ) |
|-------------|----------------------------|---|
| 10          | 3.009                      | 20  |
| 15          | 2.002                      | 30  |
| 20          | 1.5                        | 40  |
| 25          | 1.202                      | 50  |
| 30          | 1.001                      | 60  |

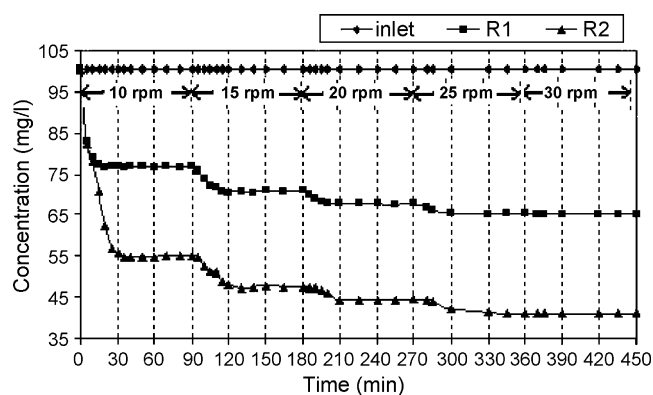


Fig. 3. Color removal of reactive red 2 dye at different speeds (pH 6.9, flow rate—100 ml/min, initial dye concentration—100 mg/l).

Experiments were carried out at 5 different speeds (10–30 rpm). The dye solution (100 mg/l) was fed continuously at constant flow rate (100 ml/min) to the reactor and the experiments were carried out for 90 min at each speed. Fig. 3 shows the results for degradation of reactive red dye at various rotational speeds. Each reactor has taken almost 30 min to reach steady state. Color removal efficiencies at different speeds are plotted in Fig. 4. The degradation rate increased with speed till 25 rpm beyond which the removal remained constant.

Low rotational speed allows the formation of a very thin liquid film over the surface, which may provide higher penetration of UV radiation and better photon utilization; on the other hand it leads to less mixing, which may cause a significant mass transfer limitation. An increase in speed increases turbulence leading to better mass transfer rates. But the disadvantage of higher speed is that it increases the water film thickness over the catalyst surface, which may reduce light intensity reaching the catalyst surface.

The results in Figs. 3 and 4 show that at slower speed the removal efficiency increased due to enhancement of mass transfer rates. The invariance of RE above a critical speed suggests

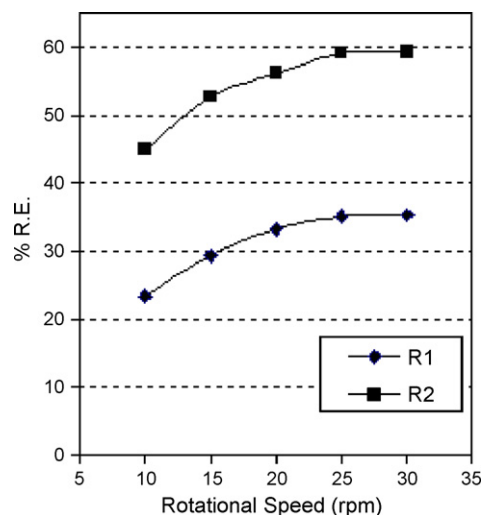


Fig. 4. Effect of rotational speed of tube on color removal of reactive red dye (pH 6.9, flow rate—100 ml/min, initial dye concentration—100 mg/l).

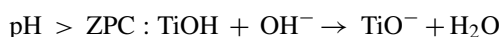
that, the reaction is not mass transfer controlled but is rather limited by the surface reaction at higher speeds.

Toyoda et al. [16] and Zhang et al. [17] have reported similar behavior of rotational speed for degradation of phenol. They suggested that it can be explained on the basis of oxidation potential of catalyst (capacity of catalyst surface to degrade certain amount of pollutant per unit time), which may be determined from the mean thickness of the liquid film over the surface, pollutant concentration and rotational speed. The rate of color removal increases when the pollutant load is less than or equal to oxidation potential of catalyst. Beyond that point it became invariant of the pollutant load.

From a practical point of view it is not advisable to operate the reactor at very high speed, as it requires more energy and costly fabrication. So an optimum speed of 25 rpm was chosen for further studies.

### 3.2. Effect of initial pH

The degradation of pollutant occurs predominantly either at the surface of  $\text{TiO}_2$  or within few monolayers around the photocatalytic surface. So adsorption of pollutant from aqueous solution on the surface of the photocatalyst is very important [18]. pH is a complex parameter since it is related to ionization state of the surface as well as that of reactant and products [19]. pH influences the surface charges of the photocatalyst. For pH's higher than zeta potential (ZPC) of titania, the surface becomes negatively charged and vice versa [20] according to following two surfacial acid–basic equilibria:



Normally the ZPC of titania is around 6.8 [21]. To study the effect of pH on reactive red dye degradation, experiments were carried out at different initial pH in the range 5–9. The optimum speed was used for these runs. The effect of pH on color removal is shown in Fig. 5. It was observed that dye removal was marginally better in acidic pH than at alkaline pH condition. Since reactive red dye is an anionic dye with sulfonate groups, which are totally ionizable in water, it becomes a negatively charged molecule, in acidic condition, where due to charge difference quick adsorption and degradation take place. Similar results were reported for Eosin by Zhang et al. [21] and for Orange G by Lachheb et al. [20].

### 3.3. Effect of initial concentration

Initial concentration of reactant plays a significant role in determining the rates of most of chemical and photochemical reactions. The degradation of reactive red dye at different initial concentrations (50–150 mg/l) is shown in Fig. 6. The optimum speed and pH were used for these runs. It was observed that as dye concentration increased the number of reactors in series increased to achieve the same extent of color removal. It was also observed that the extent of degradation decreased with increase in initial concentration of dye. The rate of removal was high

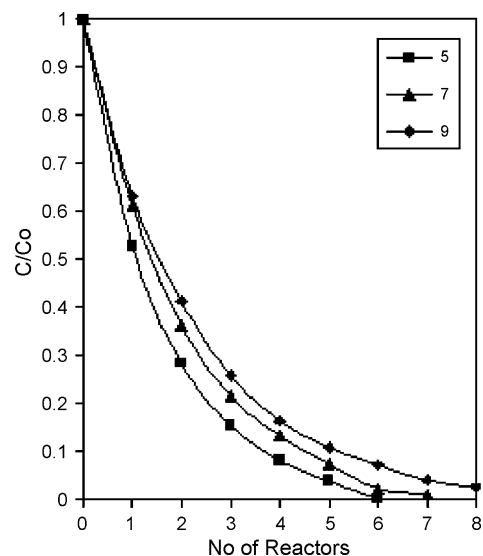


Fig. 5. Effect of initial pH on color removal of reactive red dye (flow rate—100 ml/min, initial dye concentration—50 mg/l, speed—25 rpm).

in the initial stages of reactor as seen by steeper slope. This is due to the availability of sufficient catalyst surface for dye adsorption as well as for hydroxyl radical generation at early stages. But the rate of removal slows down drastically at high concentration. Break down of dye molecules caused by hydroxyl radical attack, forms one or more intermediates, according to the complexity of the initial reactants [22]. These will also compete with dye molecule for active sites resulting in lowering the rate of color removal at later stages. Similar behavior was observed by Neepolian et al. [23] for reactive red 2 dye and by Saquib and Muneer [24] for acid green and acid red dye. Concentration of intermediates formed and absorption of photon by dye and intermediates increases at higher dye concentration resulting in lesser energy available for hydroxyl generation. Bhattacharyya et al. [25] have observed that strong adsorption intermediates

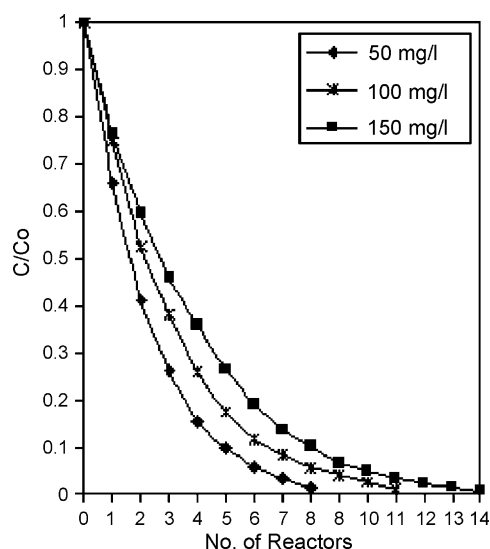


Fig. 6. Effect of initial concentration on color removal of reactive red dye (pH 5, flow rate—150 ml/min, speed—25 rpm).

Table 2

Effect of intermediates on reactive red dye removal (dye concentration—150 mg/l, speed—25 rpm, flow rate—50 ml/min)

| No of reactors | Run 1        | Run 2        | Run 3        |
|----------------|--------------|--------------|--------------|
| 0              | <b>148.1</b> |              |              |
| 1              | 74.43        | <b>74.82</b> |              |
| 2              | 30.33        | 25.15        | <b>25.78</b> |
| 3              | 14.83        | 7.03         | 5.99         |
| 4              | 6.21         | 2.87         | 0.49         |

Table 3

Effect of intermediates on reactive red dye removal (dye concentration—100 mg/l, speed—25 rpm, flow rate—150 ml/min)

| No of reactors | Run 1        | Run 2        | Run 3        | Run 4        | Run 5        |
|----------------|--------------|--------------|--------------|--------------|--------------|
| 0              | <b>109.6</b> |              |              |              |              |
| 1              | 83.08        | <b>83.03</b> |              |              |              |
| 2              | 57.50        | 56.45        | <b>56.88</b> |              |              |
| 3              | 41.80        | 36.17        | 35.40        | <b>35.50</b> |              |
| 4              | 28.51        | 25.07        | 23.10        | 21.56        | <b>21.56</b> |
| 5              | 19.16        | 15.47        | 13.88        | 11.81        | 9.86         |
| 6              | 12.80        | 10.62        | 8.56         | 7.03         | 5.35         |
| 7              | 9.21         | 6.72         | 4.98         | 3.98         | 1.89         |

formed during degradation of reactive orange II, inhibited dye degradation at later stages.

In order to get a rough idea of how much of decrease in color removal rate was due to intermediates formation, experiments were performed at constant flow rate (50 ml/min) and high concentration (150 mg/l) (where one can expect formation of more intermediates and more competition) in following manner as indicated in Table 2. The first experiment (run 1) was performed at a dye concentration of 150 mg/l in the usual manner as explained earlier. Table 2 shows the residual dye concentration of this run were 75 and 30 mg/l at the end of first and second reactor, respectively. The second run was performed with a fresh dye solution of initial concentration of 75 mg/l, which was the residual concentration at the end of first reactor and compared with first run. Similarly third run was performed with an initial dye concentration 25 mg/l and compared with second run. It was observed that run 2 and run 3 showed higher removal than run 1. This may be attributed to the higher concentration of intermediates in run 1 than in run 2. This is further conformed by comparison between run 3 and run 2.

Similar experiments were performed at lower concentration (100 mg/l) and high flow rate (150 ml/min). Results shown in Table 3 indicate that at low concentration and high flow rate the competition was slightly less, but similar trend was observed.

### 3.4. Effect of flow rate

In continuous flow reactor system, flow rate plays important role, as flow rate increases the residence time (i.e. time spent by the reactant inside the reactor) decreases. Experiments were carried out at different flow rates and results obtained are shown in Fig. 7. It can be clearly seen from the figure that an increase in flow rate increases the number of reactors in series

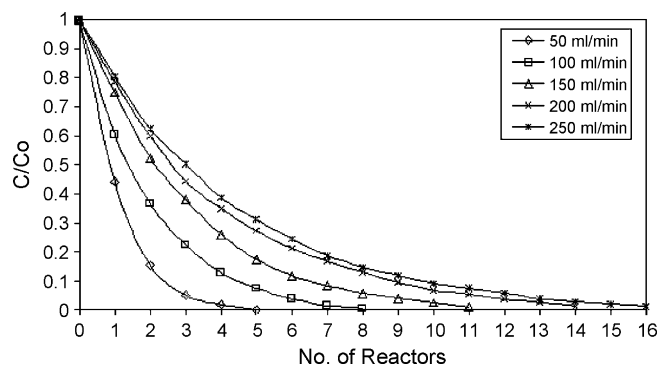


Fig. 7. Effect of flow rate on color removal of reactive red dye (pH 5, dye concentration—100 mg/l, speed—25 rpm).

for same level of color removal. The color removal per pass decreases due to insufficient residence time at higher flow rates. The same data is plotted in Fig. 8 by considering the residence time corresponding to each flow rate. It shows that lower flow rates require more time than required for higher flow rate for same extent of color removal (see Table 4) which shows that the supported catalyst is sensitive to fluid velocity. At lower flow rates due to high residence time, there is more time for reaction, which produces more intermediates. As flow rate increases the molecules spend less time in the reactor, which decreases the color removal per pass. However, at very high flow rate the total dye load increases and hydroxyl radicals produced may be insufficient to oxidize them resulting in poor removal. Al-Ekabi and Serpone [26] have observed that the rate of phenol degradation in TiO<sub>2</sub> coated tubular reactor increases nonlinearly with flow rate, reaching a plateau at higher flow.

The effect of flow rate may also be compared on the basis of energy consumption, which was calculated from the rated wattage of lamp (KW) used and reaction time ( $t$ ) ( $\text{KW h/l} = \text{KW} \times t/V_{\text{reactor}}$ ). Energy consumption at different flow rates and dye concentrations is given in Table 4. Fig. 9 shows the surface contour plot for the effect of flow and concentration on energy consumption. It was observed that energy consumption increased with increase in concentration at each flow rate. However energy consumption decreased (by 30–33%) with increase in flow rate up to some level and then increased

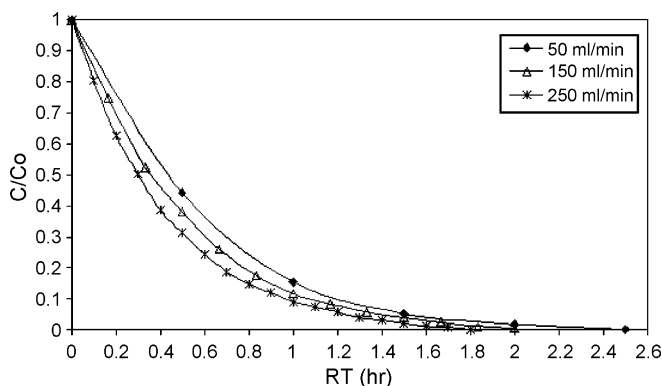


Fig. 8. Effect of flow rate on color removal of reactive red dye (pH 5, dye concentration—100 mg/l, speed—25 rpm).



Table 4  
Energy consumption at different flow rate and concentration

| Concentration (mg/l) | Flow rate (ml/min) | No. of reactors | RE (%) | Time (min) | Energy consumption (EC) (kW h/l) | EC (%) |
|----------------------|--------------------|-----------------|--------|------------|----------------------------------|--------|
| 50                   | 50                 | 4               | 99.97  | 120        | 0.06000                          | 100.00 |
|                      | 100                | 6               | 99.99  | 90         | 0.04500                          | 75.00  |
|                      | 150                | 8               | 98.98  | 80         | 0.04000                          | 66.67  |
|                      | 200                | 11              | 99.29  | 82.5       | 0.04125                          | 68.75  |
|                      | 250                | 14              | 99.18  | 84         | 0.04200                          | 70.00  |
| 100                  | 50                 | 5               | 99.98  | 150        | 0.07500                          | 100.00 |
|                      | 100                | 8               | 99.36  | 120        | 0.06000                          | 80.00  |
|                      | 150                | 12              | 99.27  | 120        | 0.06000                          | 80.00  |
|                      | 200                | 15              | 99.12  | 112.5      | 0.05625                          | 75.00  |
|                      | 250                | 18              | 99.21  | 108        | 0.05400                          | 72.00  |
| 150                  | 50                 | 7               | 99.33  | 210        | 0.10500                          | 100.00 |
|                      | 100                | 11              | 99.51  | 165        | 0.08250                          | 78.57  |
|                      | 150                | 15              | 99.31  | 150        | 0.07500                          | 71.43  |
|                      | 200                | 19              | 99.62  | 142.5      | 0.07125                          | 79.17  |
|                      | 250                | 24              | 99.76  | 144        | 0.07200                          | 80.00  |

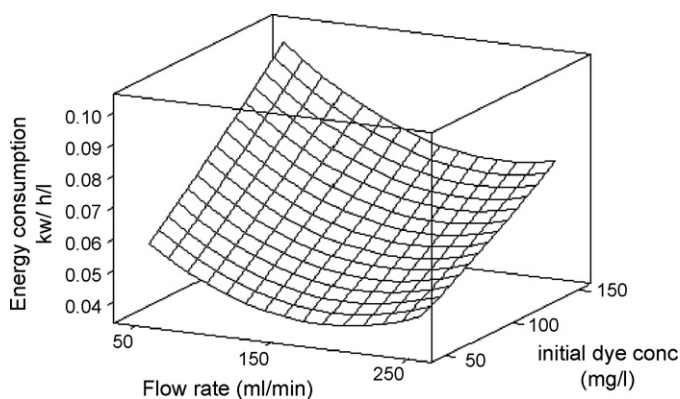


Fig. 9. Contour surface plot for energy consumption at different concentration.

slightly at higher flow rates for all the concentration. The energy consumption data for different flow rates is presented in Table 5 for an initial concentration of 100 mg/l. It clearly shows that initial 50% of total energy consumption results in nearly 85% of dye removal and the remaining 15% dye removal take additional 50%.

### 3.5. Kinetics of decolorization

Since the reactors in series approach has been used for studying the decolorization, the plug flow model given in Eq. (1) can be applied for the kinetics of decolorization. Where  $C$  is dye concentration at time  $t$  and  $C_0$  is initial dye concentration and  $\tau$  is residence time. In the literature, rate expressions from simple pseudo first order kinetic model to more complex expressions based on adsorption and reaction have been used. The photocatalytic oxidation kinetics of many organic compounds has often been modeled with the Langmuir–Hinshelwood rate kinetic given in Eq. (2) [27]. Solving these two equations we get Eq. (3). The experimental data for each flow rate were fitted to Eq. (3) and values of  $k_r$  the reaction rate constant, and  $K$  the adsorption coefficient were calculated from linear fit. Fig. 10 shows the linear fit for 50 and 200 ml/min flow rate. Table 6 shows the values of  $k_r$  and  $K$ . Results showed that the rate constant increased with increase in flow rate.

$$\tau = - \int_{C_0}^C \frac{dC}{r} \quad (1)$$

Table 5  
Energy consumption at different flow rates

| Concentration mg/l | Flow rate ml/min | R.T. hr | No. of Reactors | R.E. %       | Energy consumption (EC) KW.h/l | % EC      |
|--------------------|------------------|---------|-----------------|--------------|--------------------------------|-----------|
| 100                | 50               | 0.5     | 2               | <b>84.51</b> | 0.030                          | <b>40</b> |
|                    |                  |         | 4               | 98.21        | 0.060                          | 80        |
|                    |                  |         | 5               | 99.98        | <b>0.075</b>                   | 100       |
|                    | 100              | 0.25    | 2               | 63.21        | 0.015                          | 25        |
|                    |                  |         | 4               | <b>87.13</b> | 0.030                          | <b>50</b> |
|                    |                  |         | 6               | 96.01        | 0.045                          | 75        |
|                    | 150              | 0.1667  | 8               | 99.36        | <b>0.060</b>                   | 100       |
|                    |                  |         | 2               | 47.53        | 0.010                          | 16        |
|                    |                  |         | 4               | 73.98        | 0.020                          | 33        |
|                    |                  |         | 6               | <b>88.32</b> | 0.030                          | <b>50</b> |
|                    |                  |         | 8               | 94.27        | 0.040                          | 66        |
|                    |                  |         | 10              | 97.32        | 0.050                          | 83        |
|                    |                  |         | 12              | 99.27        | <b>0.060</b>                   | 100       |

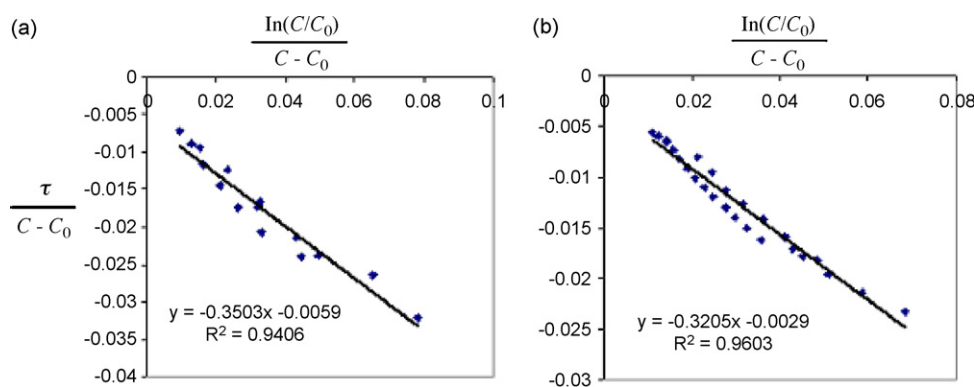


Fig. 10. Kinetic parameter estimation using L–H kinetic model at two different flow rates (a) 50 ml/min and (b) 200 ml/min.

Table 6  
Effect of flow rates on L–H kinetic parameters

| Flow rate (ml/min) | $K$ (l/mg) | $k_r$ (mg/l/h) | $R^2$ (linear fit) |
|--------------------|------------|----------------|--------------------|
| 50                 | 0.0168     | 169.49         | 0.9401             |
| 100                | 0.0105     | 303.10         | 0.9048             |
| 150                | 0.0092     | 322.01         | 0.8901             |
| 200                | 0.0090     | 340.00         | 0.9603             |

$$r = \frac{k_r KC}{1 + KC} \quad (2)$$

$$\frac{\tau}{C - C_0} = -\frac{1}{k_r K} \left( \frac{\ln(C/C_0)}{C - C_0} \right) - \frac{1}{k_r} \quad (3)$$

### 3.6. Degradation of dyes

The degradation of dye was also studied by measuring TOC removal and nearly 55–70% of TOC was removed by photocatalytic oxidation. Total oxidation of any contaminant proceeds through one or more intermediates, according to the complexity of the initial reactants [22]. The absorbance spectrum of reactive red dye samples taken at different reaction times showed a gradual and complete disappearance of the peak corresponding to the chromophoric azo group of the dye ( $\lambda = 545$  nm). The conductivity of solution was increased from  $\sim 150$  to  $\sim 300$  mS/cm which indicated mineralization of hetero atoms present in the dye, such as sulfur into sulfate ions and nitrogen atom into ammonium and nitrate. Evolution of these ions may have increased the conductivity. Guillard et al. [28] have also observed formation of these ions for four different dyes and the rate of formation of each ion was different for different dyes.

## 4. Conclusion

Studies on photocatalytic degradation of reactive red dye using an immobilized rotating tube photocatalytic reactor, immobilized with  $\text{TiO}_2$ , exposed to UV tubes showed that nearly 90–99.9% color removal and 55–70% TOC removal was obtained depending on the initial dye concentration and

exposure time. Initial concentration of dye plays a significant role in dye degradation with the low initial concentration giving better color removal. Dye degradation was also a function of pH with acidic pH favoring the color removal. Rate of color removal increased with increase in rotational speed up to 25 rpm and then remained constant. Flow rate has a significant effect on color removal and energy consumption.

## References

- [1] M.R. Hoffmann, S.T. Martin, W. Choi, D.W. Bahnemann, Chem. Rev. 95 (1995) 69–96.
- [2] A. Mills, S.L. Hunte, J. Photochem. Photobiol. A: Chem. 108 (1997) 1–35.
- [3] D.F. Ollis, C. Turchi, Environ. Prog. 9 (1990) 229–234.
- [4] T.Y. Wei, C.C. Wan, Ind. Eng. Chem. Res. 30 (1992) 1293–1300.
- [5] J.M. Herrmann, C. Guillard, P. Pichat, Catal. Today 17 (1993) 7–20.
- [6] P.S. Mukherjee, A.K. Ray, Chem. Eng. Technol. 22 (1999) 253–260.
- [7] D.D. Dionysiou, A.P. Khodadoust, A.M. Kern, M.T. Suidan, I. Baudin, J.M. L  n  , Appl. Catal. B: Environ. 24 (3–4) (2000) 139–155.
- [8] F. Chen, Y. Xie, J. Zhao, G. Lu, Chemo. 44 (5) (2001) 1159–1168.
- [9] R.L. Pozzo, M.A. Baltanas, A.E. Cassano, Catal. Today 39 (1997) 219–231.
- [10] A.K. Ray, Chem. Eng. Sci. 54 (1999) 3113–3125.
- [11] A.K. Ray, Catal. Today 44 (1998) 357–368.
- [12] A.K. Ray, A.C.M. Beenackers, Catal. Today 40 (1998) 73–83.
- [13] T.K. Sengupta, M.F. Kabir, A.K. Ray, Ind. Eng. Chem. Res. 40 (2001) 5268–5281.
- [14] D.D. Dionysiou, G. Balasubramanian, M.T. Suidan, A.P. Khodadoust, I. Baudin, J.M. L  n  , Water Res. 34 (11) (2000) 2927–2940.
- [15] D.D. Dionysiou, M.T. Suidan, I. Baudin, J.M. Laine, Appl. Catal. B: Environ. 38 (2002) 1–16.
- [16] A. Toyoda, L. Zhang, T. Kanki, N. Sano, J. Chem. Eng. Japan 33 (1) (2000) 188–191.
- [17] L. Zhang, T. Kanki, N. Sano, A. Toyoda, Solar Energy 70 (4) (2001) 331–337.
- [18] M.A. Hasnat, I.A. Siddiquey, A. Nuruddin, Dyes Pigm. 66 (2005) 185–188.
- [19] A. Houas, H. Lachheb, M. Ksibi, E. Elaloui, C. Guillard, J.-M. Herrmann, Appl. Catal. B: Environ. 31 (2001) 145–157.
- [20] H. Lachheb, E. Puzenat, A. Houas, M. Ksibi, E. Elaloui, C. Guillard, J.-M. Herrmann, Appl. Catal. B: Environ. 102 (2002) 1–16.
- [21] F. Zhang, J. Zhao, T. Shen, H. Hidaka, E. Pelizzetti, N. Serpone, Appl. Catal. B: Environ. 15 (1998) 147–156.

- [22] D.F. Ollis, *Surf. Chem. Catal.: Chem.* 3 (2000) 405–411.
- [23] B. Neepolian, M. Shankar, V.V. Murugesan, *J. Sci. Ind. Res.* 61 (2002) 224–230.
- [24] M. Saquib, M. Muneer, *Coloration Tech., Soc. Dyers Colourists* 118 (2002) 307–315.
- [25] A. Bhattacharyya, S. Kawi, M.B. Ray, *Catal. Today* 98 (3) (2004) 431–439.
- [26] H. Al-Ekabi, N. Serpone, *J. Phys. Chem., Am. Chem. Soc.* 92 (20) (1998) 5726–5731.
- [27] C.S. Turchi, D.F. Ollis, *J. Catal.* 122 (1) (1990) 178–192.
- [28] C. Gulliard, H. Lachheb, A. Houas, M. Ksibi, E. Elaloui, J.-M. Herrman, *J. Photochem. Photobiol. A: Chem.* 158 (2003) 27–36.